Heading Estimation for Autonomous Robot Using Dual-Antenna GPS

Tien-Dung Quoc Tran and Vinh-Hao Nguyen
Ho Chi Minh City University of Technology, Vietnam
Email: tqtiendung@hcmut.edu.vn, vinhhao@hcmut.edu.vn

***Abstract*—Most of the attitude estimation systems are built from inertial measurement units (IMUs). Micro-electro-mechanical system-based (MEMS) IMUs are low-cost but large errors. MEMS-based angle estimator often uses a tri-axis magnetometer to determine the yaw angle (heading angle) that the estimation accuracy is significantly influenced by the stability of the environment's magnetic field. This paper introduces a new method to estimate the heading angle using Global Positioning System (GPS) with dual-antenna. The proposed estimation algorithm is independent of the magnetic field and has high accuracy in the heading angle. Through experiments, we also show that the heading accuracy depends on the quality of the GPS receivers and the antennas.**

***Index Terms*—Global Positioning System (GPS), real-time kinematic (RTK), heading estimation**

I. Introduction

Nowadays there are a lot of dangerous working environments for people such as mountains, deserts, radioactive areas, etc. Autonomous vehicle is the reasonable solution for these problems. In order for the robot to operate stably and efficiently, navigation is one of the important issues that need to be addressed. There are many positioning methods for autonomous robots and can be divided into three main methods: dead-reckoning, using landmarks and positioning using maps. Dead-reckoning method uses inertial measurements such as velocity, acceleration, angular rate to determines the vehicle's displacement from previous sampling epoch. In the method of positioning using landmark, the sensor measures the distance (and possibly the bearing angle) between the vehicle and the landmarks, thereby applying calculations to infer the vehicle's position. In the last method, the robot uses distance sensors to determine the features of the surrounding environment, compare with the map saved in its memory to determine its position. These methods have their own advantages and disadvantages, such as the dead-reckoning method gives high accuracy results in a short time, but the estimated error will be accumulated quickly over time, especially in the case of using low-cost inertial sensors [1]. In order to take advantage of the above integrated methods, we combine sensors together by using sensor fusion algorithm. The algorithm of combining Global Navigation Satellite System (GNSS) and Inertial Navigation System (INS) is widely considered.

The attitude estimation mostly depends on the IMU. Paper [2] indicates that we can use IMU to determine orientation by integrating angular velocity, combining with tri-axis accelerometer and magnetometer to reduce error. For low-cost IMUs, the accuracy is still limited. MEMS-based IMUs often have large sensor biases, so if there is not an accurate sensor calibration method, the estimation result of the rotation angle is not good. In [3], E.H. Shin developed an INS/GPS navigation system and proposed the MEMS IMU calibration procedure and method, resulting in a significantly reduced sensor drift. We can use magnetometer to reduce heading estimation errors. However, the accuracy decreases when the environment has large magnetic disturbances. We can also use some other types of sensor such as stereo camera, LiDAR, etc. [4], [5]. Alatise in [4] presented a new method combining IMU with a camera, using Extended Kalman Filter to estimate Euler angles. The heading angle RMS error when using this algorithm is 0.2 degrees with an estimated stabilization time of 3 minutes.

When we use low-cost IMUs, estimated position and velocity often have large cumulative errors over time. In addition, INS system cannot self-determine the initial state of the vehicle. To solve these problems, Global Positioning System (GPS) is combined to eliminate the accumulated errors of the estimator. However, GPS has some disadvantages like low updating rate, sometimes the satellites' signal is suspended. Gao et al. built an integrated navigation system using IMU, GPS and LiDAR sensors, which can be switched between GPS when operating in opening spaces or LiDAR in GPS restricted areas [6]. Another method is to build a tightly-coupled GPS/INS system. Angrisano built a tightly-coupled system, in which the estimator does not use position and velocity received from GPS module but uses raw measurements including pseudorange and Doppler measurements to estimate continuously even when the number of received signals is smaller than 4 [7]. In the above research, authors only use GPS to estimate IMU sensor biases, not to estimate heading angle.

Real-time Kinematic (RTK) is a method to improve the accuracy of the GPS navigation system based on differential calculations. According to [8], the signal from satellite is disturbed when transmitting in Earth's atmosphere (tropospheric and ionospheric error). Some

Manuscript received February 1, 2020; revised October 11, 2020

doi: 10.18178/ijmerr.9.12.1566-1572

other kinds of GPS errors are multipath error and time asynchronous error between the satellite's clock and the receiver's clock. This paper also pointed out that using single-difference (SD) can eliminate discrepancies between receivers or satellites and using double-difference (DD) can eliminate discrepancies between receivers and satellites. The RTK model requires two GPS receivers (base and rover station) that can determine the position of a vehicle with centimeter-level accuracy. With such high accuracy, a multi-receiver system can be used to determine the heading angle of a vehicle. Consoli et al. presented the model of a heading estimation system that uses multiple GPS receivers [9]. However, this paper only presented the ideas and simulated the effect when changing the baseline length. Papers [10] and [11] introduced a model using multiple GPS receivers to determine rotation angle and showed the simulation results. In [12], the authors combined a high-precision IMU and two GPS receivers, including a high-precision receiver and a low-cost one. This system obtained an accuracy of 0.2 degrees for heading angle with a baseline of 92 centimeters.

This paper consists of three sections. The first section presents the method of determining the heading angle using dual-antenna GPS, including two main steps: determining the position by the Differential GPS (DGPS) method and solving the ambiguity integer problem using LAMBDA/MLAMBDA algorithm. The next section shows the experimental setup for testing. There are two kinds of testing system: single-frequency receiver (can receive only 1 type of carrier signal) and dual-frequency (can receive up to 2 types of carrier signal). The micro-processor used for both systems is the ARM Cortex-M7 processor. The last section shows test results (including static test and dynamic test) and conclusions.

II. METHOD

GPS was the first worldwide established GNSS (Global Navigation Satellite System) system in the 1970s. In the beginning, GPS was only used for military purposes, but it is now available for civil purposes with certain restrictions. From the received signals, GPS receiver can determine the distance to the satellite and satellite's position. Therefore, we can determine the position of the receiver. The accuracy of this measurement is about 2 meters.

The heading angle estimation system from dual-antenna GPS uses code phase (also known as pseudorange) and carrier phase measurement. Pseudorange measurement taken from GPS C/A code whose frequency of 1.023 MHz. The signal frequencies of carrier phase measurement method are much larger (1575.42 MHz with L1, 1227.60 MHz with L2 and 1176.45 MHz with L5). Therefore, pseudorange measurement is less accurate. The power of the noise in the carrier phase measurement is approximate 10 times less. However, there is a disadvantage that the measurement has an integer ambiguity. It means the measured value of the carrier measurement is different from the correct value by an integer N cycle(s).

Originally, the principle of the RTK algorithm was that the base station was stationary, from the difference between base and rover in carrier phase measurements and pseudorange measurements, we can calculate the position of the rover. The RTK positioning method can achieve centimeter-level accuracy. In determining the heading angle based on the GPS, both base and rover antennas are mounted on the vehicle and are moving. In this case we use single point positioning method based on pseudorange measurement to determine the base station's position. After that, we use the RTK algorithm to estimate the high-accuracy position of rover. This method is called moving base RTK. This method only focuses on the relative position between base and rover antennas, and the position accuracy is low because the single point positioning method using pseudorange measurements which have large disturbance. Another method is presented in [13], GPS-RTK algorithm uses pseudorange measurements and Kalman filter to approximate base and rover positions, thereby using carrier phase measurements to correct the position results.

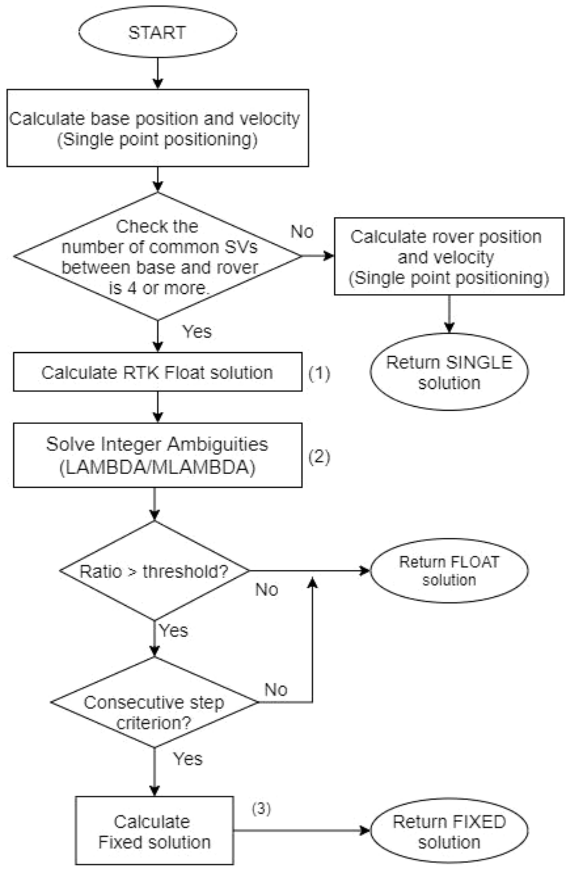

Figure 1. Flowchart of GPS Real-time kinematic algorithm.

The flowchart of the GPS-RTK algorithm is shown in Fig. 1, which can be divided into three steps (numbered from (1) to (3) on the flowchart). First, we calculate the differential GPS (DGPS) position (float solution). The DGPS solution has low accuracy of 1 meter. Next, we solve the optimization problem using the algorithm LAMBDA/MLAMBDA to determine the ambiguity integer values of the carrier phase measurements. Finally, we determine the high-accuracy position of the rover (fixed solution).

A. Calculate DGPS Solution Using Kalman Filter and Single Differences

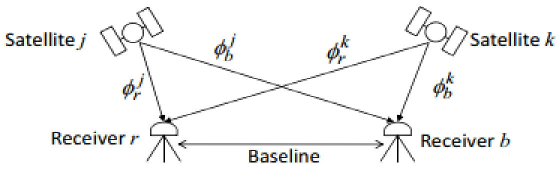

Figure 2. Illustration of the GPS-RTK algorithm.

To calculate the float solution, we can use the Extended Kalman Filter. The state vector consists of the position, velocity of the rover station and single differences of the integer ambiguities. At this time, GPS receivers support up to 3 carrier frequencies (L1, L2 and L5). For each frequency we have a carrier phase integer ambiguity value. Since current GPS system has 32 satellites, the length of state vector when we use 1, 2, 3 frequencies will be 38, 70 and 102, respectively. Generally, in this paper we present equations for triple-frequency case. If the GPS receiver uses less than 3 frequencies, we will eliminate the corresponding components. We have the state vector:

$$x_k = \left[r_r(k) \quad v_r(k) \quad B^i_{rb,L1}(k) \quad B^i_{rb,L2}(k) \quad B^i_{rb,L5}(k) \right]^T \quad (1)$$

The formula for calculating DD of carrier and pseudorange measurements is as follows (used for all carrier frequencies).

$$\Phi^{ij}_{rb,Lx} = \rho^{ij}_{rb} + \lambda_x \left(B^i_{rb,Lx} - B^j_{rb,Lx} \right) + \varepsilon_\Phi \quad (2)$$

$$P^{ij}_{rb} = \rho^{ij}_{rb} + \varepsilon_P \quad (3)$$

$$\rho^{ij}_{rb} = \rho^i_{rb} - \rho^j_{rb} = \left(\rho^i_r - \rho^i_b \right) - \left(\rho^j_r - \rho^j_b \right) \quad (4)$$

where ρ^{ij}_{rb} is the DD of the geometric range between satellites i, j and receivers base (b), rover (r). λ_x (x = 1, 2, 5) is the wavelength corresponding to the GPS carrier frequency. ε_Φ and ε_P are measurement noise. Similarly, we can calculate the other DD components. There are many sources of disturbances that affect to the GPS measurements, such as clock bias, clock drift of the receivers and satellites, errors due to the signal passing through the environment (ionospheric delay and tropospheric delay), multipath errors, etc. The differential method has the advantage of reducing these errors, the other sources of unspecified noise can be modeled as white noise. The variance of measurement noise can be calculated by the following formula:

$$\sigma^2_{sat} = 2 f_{PR/CP} \left(a^2 + \frac{b^2}{\sin(El)} \right) \quad (5)$$

where $f_{PR/CP}$ is the ratio of pseudorange error to carrier phase measurement error. El is the elevation angle of satellite relative to receiver. According to Eq. (5), the greater the elevation angle, the bigger the measurement error. So we choose the reference satellite to calculate the double differences is the satellite with the largest elevation angle. In addition, we remove measurements to satellites whose elevation angles less than a predetermined threshold to avoid causing large errors in the estimation results. The measurement model includes carrier phase and pseudorange measurements:

$$y_k = \left[\Phi^{ki}_{rb,L1} \quad P^{ki}_{rb,L1} \quad \Phi^{ki}_{rb,L2} \quad P^{ki}_{rb,L2} \quad \Phi^{ki}_{rb,L5} \quad P^{ki}_{rb,L5} \right]^T_{(6m-6)\times 1} \quad (6)$$

where k is the index corresponding to the reference satellite, m is the number of satellites from which both the rover and base can receive signal, i is the number running from 1 to m and is not equal to k. From (6), we have the measurement model equation:

$$z = h(x_k) = \begin{bmatrix} \rho^{ki}_{rb,L1} + \lambda_1 \left(B^k_{rb,L1} - B^i_{rb.L1} \right) \\ \rho^{ki}_{rb,L1} \\ \rho^{ki}_{rb,L2} + \lambda_2 \left(B^k_{rb,L2} - B^i_{rb.L2} \right) \\ \rho^{ki}_{rb,L2} \\ \rho^{ki}_{rb,L5} + \lambda_5 \left(B^k_{rb,L5} - B^i_{rb.L5} \right) \\ \rho^{ki}_{rb,L5} \end{bmatrix}_{(6m-6)\times 1} \quad (7)$$

We have the linearized measurement matrix H:

$$H = \begin{bmatrix} -DE & 0 & \lambda_1 D & 0 & 0 \\ -DE & 0 & 0 & 0 & 0 \\ -DE & 0 & 0 & \lambda_2 D & 0 \\ -DE & 0 & 0 & 0 & 0 \\ -DE & 0 & 0 & 0 & \lambda_5 D \\ -DE & 0 & 0 & 0 & 0 \end{bmatrix} \quad (8)$$

The rows of matrix E (m rows, 3 columns) are the line-of-sight unit vector from the receiver to m satellites. Matrix D (m-1 rows, m columns) represents the calculation of DD. Using Eq. (9), we obtain the float solution of the algorithm:

$$\begin{cases} K = P^- H^T \left(H P^- H^T + R \right)^{-1} \\ x^+ = x^- + K\left(y - h\left(x^-\right) \right) \\ P^+ = \left(I_{(3m+6)\times(3m+6)} - KH \right) P^- \end{cases} \quad (9)$$

B. Solve the Integer Ambiguity Using LAMBDA/ MLAMBDA Algorithm

To determine the high-accuracy position (fixed solution), we convert single difference to double difference by the following formula:

$$\begin{cases} \hat{x}'_k = G \hat{x}_k = \begin{bmatrix} \hat{r}_r \\ \hat{v}_r \\ \hat{N} \end{bmatrix}_{(3m+3)\times 1} \\ P'_k = G P_k G^T = \begin{bmatrix} Q_R & Q_{NR} \\ Q_{RN} & Q_N \end{bmatrix} \end{cases} \quad (10)$$

In Eq. (10), G is the SD to DD transform matrix, $\hat{N}$ is a vector consist of the double differences of carrier phase ambiguity and Q_N is the corresponding estimation covariance matrix. In fact, we know that the values of N are integers, which leads to an integer optimization problem to find the optimal vector $\breve{N}$:

$$\breve{N} = \operatorname{argmin}\left(N-\hat{N}\right)^T Q_N^{-1}\left(N-\hat{N}\right) \tag{11}$$

This optimization problem has no specific empirical formula, we can only use search algorithms to find the optimal solution. A method to find the optimal solution for this problem is given by Teunissen called LAMBDA (Least-squares Ambiguity Decorrelation Adjustment) [14]. After that, X.-W. Chang et al. improved the method and name it MLAMBDA (Modified LAMBDA) whose advantages of decrease search time and improve computational performance [15]. The current methods will consist of two steps. First, we restrict the search set to a hyper ellipsoid. After that, we use the brute force method to search across all elements of the restricted set. In order to verify the quality of the optimal solution, the algorithm also finds a second optimal solution N_2. The ratio-test value R is:

$$R = \frac{\left(N_2-\hat{N}\right)^T Q_N^{-1}\left(N_2-\hat{N}\right)}{\left(\breve{N}-\hat{N}\right)^T Q_N^{-1}\left(\breve{N}-\hat{N}\right)} \tag{12}$$

The estimated values of $\hat{N}$ and Q_N can be affected by noise, the solution obtained from this algorithm is not yet certain to be the true value of the double difference of the carrier phase integer ambiguity. The larger R value, the greater the accuracy of the solution. Normally we choose the threshold value is 3. If R is greater than threshold value, we calculate the fixed solution and errors of RTK algorithm by the formula:

$$\begin{bmatrix}\breve{r}_r \\ \breve{v}_r\end{bmatrix} = \begin{bmatrix}\hat{r}_r \\ \hat{v}_r\end{bmatrix} - Q_{RN}Q_N^{-1}\left(\hat{N}-\breve{N}\right) \tag{13}$$

$$\breve{Q}_R = Q_R - Q_{NR}Q_N^{-1}Q_{RN} \tag{14}$$

Initial values of the integer ambiguities often have large deviations from the correct values, therefore sometimes the first fixed solution is incorrect. To solve this problem, we use consecutive fixed constraint. According to this method, the estimator determines the result to be fixed if and only if the ratio R is greater than the threshold for at least 10 consecutive epochs, otherwise the solution quality is only float. In addition to the aforementioned method, there are some other algorithms to enhance estimation quality such as cycle slip detection, hold integer ambiguities, etc. From the estimated positions in ECEF (Earth-Centered Earth-Fixed) frame, we calculate the vector from base to rover in NED (North-East-Down) frame:

$$r_{rb}^n = \begin{bmatrix} -s_\varphi c_\lambda & -s_\lambda & -c_\varphi c_\lambda \\ -s_\varphi s_\lambda & c_\lambda & -c_\varphi s_\lambda \\ c_\varphi & 0 & -s_\varphi \end{bmatrix}\left(r_r^e - r_b^e\right) \tag{15}$$

where r_r^e, r_b^e are the estimated positions of rover and base, respectively. λ, φ are the longitude and latitude of base station. Denote θ for pitch angle, ψ for heading angle, d for the distance between antennas, we have the below equation:

$$r_{rb}^n = \begin{bmatrix} r_{rb,N}^n \\ r_{rb,E}^n \\ r_{rb,D}^n \end{bmatrix} = \begin{bmatrix} d\cos\theta\cos\psi \\ d\cos\theta\sin\psi \\ -d\sin\theta \end{bmatrix} \tag{16}$$

We can calculate the angles and baseline by:

$$\begin{aligned} d &= \left\| r_{rb}^n \right\|, \psi = \arctan 2\left(r_{rb,E}^n, r_{rb,N}^n\right), \\ \theta &= \arcsin\left(-\frac{r_{rb,D}^n}{d}\right), d_{baseline} = d\cos\theta \end{aligned} \tag{17}$$

III. Experiment Setup

The block diagram of the dual-antenna GPS system is shown in Fig. 3. GPS receivers are not required to be the same. However, we should use the same type of receivers for both base and rover since the same error characteristics of the receivers can be eliminated.

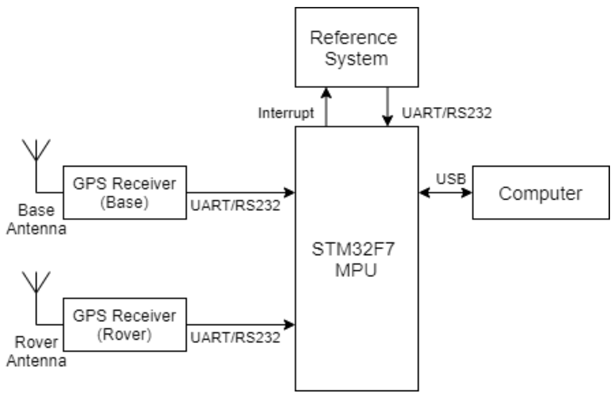

Figure 3. Block diagram of the dual-antenna GPS system.

The receivers communicate with the central microprocessor via serial communication standards like RS232 or UART. The central microprocessor used is the STM32F767ZI from STMicroelectronics. This processor used ARM Cortex-M7 core with a high-speed clock frequency of 216 MHz and it supports double-precision floating-point unit (64-bit floating-point). Estimation results are sent to the computer via USB port. The software used for collecting data between the computer and GPS-RTK system is programmed in C# programming language. This user interface allows us to collect and display data, plot graphs, calculate RMS errors and log data for post-processing.

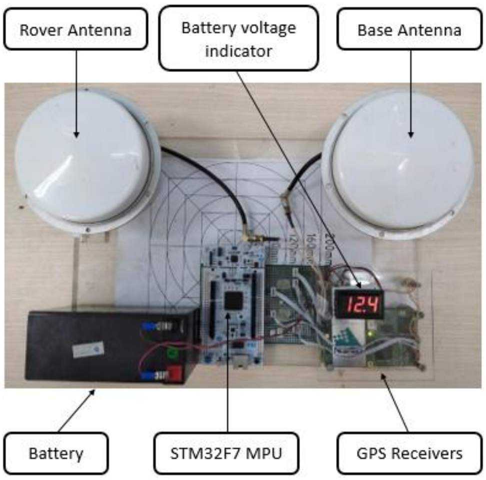

Figure 4. Heading estimation system using dual-frequency receivers.

In static test case, we nailed two antennas at distances of approximately 0.3, 0.5, 1 and 2 meters to determine the relation between static error and baseline distance. For the dynamic test, we use the slider system shown in Fig. 5. The base's antenna is fixed and rover's antenna is placed on the slider. The slider system's maximum travel length is 0.6 meters and maximum moving speed is about 0.4 m/s.

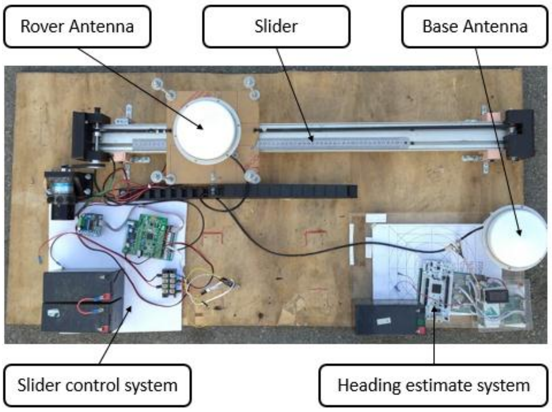

Figure 5. Slider system in the dynamic test.

IV. Results

A. Static Test

As mentioned above, the principle of the static test method is that we fixed two antennas with baseline distances of approximately 0.3, 0.5, 1 and 2 meters. The sampling frequency is set to 5 Hz for both base and rover receivers. The calculation time for each epoch is about 50 milliseconds. We determine the relation between the baseline and the ratio of the fixed solution and the RMS error of the heading angle estimation. We have the following result in TableI and Table II.

From the result tables, we can conclude that using dual-frequency receivers gives much better results than single-frequency receivers (69% versus 60%). In some cases, single-frequency system cannot find any fixed solution (dataset number 1 and 4). Regarding heading angle errors, the RMS errors are smaller when baseline increases for both types of receivers. Theoretically, the position's horizontal error of the GPS-RTK algorithm is almost constant when the baseline is small (only changes a few parts per million of the baseline). We can see in Fig. 6, when we increase the distance between the antennas, the heading estimation error will be smaller. Comparing between the two types of GPS receivers, we can see that with the same baseline length, the dual-frequency will give a smaller error than the single-frequency receiver.

TABLE I. Test Results (Single-Frequency Receiver)

Dataset number	Average estimated baseline (m)	Baseline RMS error (m)	Heading standard deviation (degree)	Number of received message	Fix ratio (%)
1	No fixed solution				
2	0.2797	0.0041	1.1011	3988	76.05
3	0.2773	0.0036	0.9804	2741	82.09
4	No fixed solution				
5	0.5212	0.0027	0.6321	6484	80.77
6	0.5187	0.003	0.3589	5059	64.6
7	1.0049	0.0023	0.1303	5894	9.14
8	1.0077	0.0027	0.1828	5504	62.63
9	1.0047	0.004	0.2135	5232	38.67
10	1.986	0.0035	0.1227	8348	90.11
11	1.9851	0.003	0.0903	5770	21.66
12	1.9841	0.0029	0.082	4708	84.3

TABLE II. Test Results (Dual-frequency Receiver)

Dataset number	Average estimated baseline (m)	Baseline RMS error (m)	Heading standard deviation (degree)	Number of received message	Fix ratio (%)
1	0.298	0.002	0.6692	1518	66.14
2	0.2846	0.0038	0.521	1094	49.82
3	0.2902	0.0035	0.5186	1193	84.33
4	0.2813	0.0039	0.5538	972	83.33
5	0.5004	0.003	0.3365	1918	52.24
6	0.4992	0.0022	0.2226	1094	80.16
7	1.0336	0.0048	0.1568	1850	54.05
8	1.0126	0.0033	0.138	1004	99.9
9	1.019	0.0027	0.132	722	19.25
10	2.008	0.003	0.0762	1011	99.31
11	2.0058	0.0041	0.0823	1006	99.7
12	2.045	0.0032	0.0753	1012	54.84

Denote σ for horizontal error of the estimator, $d_{baseline}$ for baseline distance, we have the formula of heading error:

$$\Delta\psi = \arcsin\left(\frac{\sigma}{d_{baseline}}\right) \approx \frac{\sigma}{d_{baseline}} \tag{18}$$

Usually, the baseline length is much greater than the horizontal error of the GPS-RTK positioning system ($d_{baseline} >> \sigma$). According to Eq. (18), heading errors decrease when horizontal precision increases or baseline distance increases. From the datasheet of the receivers, we see that the accuracy of the dual-frequency receiver used in this experiment is 1 cm + 1 ppm, smaller than the error of single-frequency receiver (2.123 cm + 1 ppm), that is the reason why when the same baseline value, the dual-frequency receiver gives better estimation performance. From the above formula, we also see that the larger the baseline length, the angle error is inversely proportional to the baseline. So if the baseline is bigger, the accuracy is better.

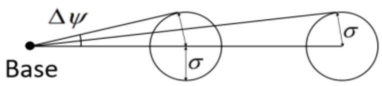

Figure 6. Relation between baseline and estimation error.

From the results in Table I, Table II and Eq. (18), we have the graph of RMS error of the heading angle according to baseline distance (Fig. 7). The coefficients of the curve were estimated by the least square error method.

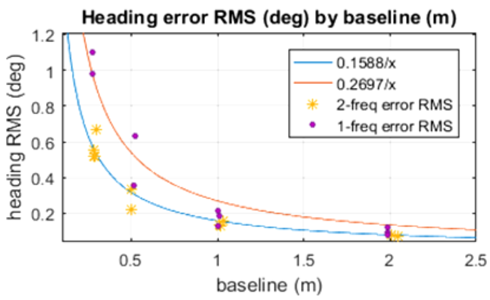

Figure 7. Relative of the heading RMS error by baseline distance.

In addition to heading angle estimation, we also consider the position estimation (to apply in the GPS/INS integrated navigation system). From Fig. 8 and Fig. 9, we can see that the moving base RTK measurement does not increase the absolute position accuracy of the vehicle, it only ensures the relative position accuracy on Earth Geographical coordinate system. We can conclude that the RTK algorithm with 2 antennas can only achieve high accuracy position or high accuracy heading angle. In order to increase both the accuracy of position and heading angle, we have to use at least three antennas. In that case, an antenna is a fixed base to increase position accuracy, the other two antennas are mounted in the vehicle for calculating heading angle.

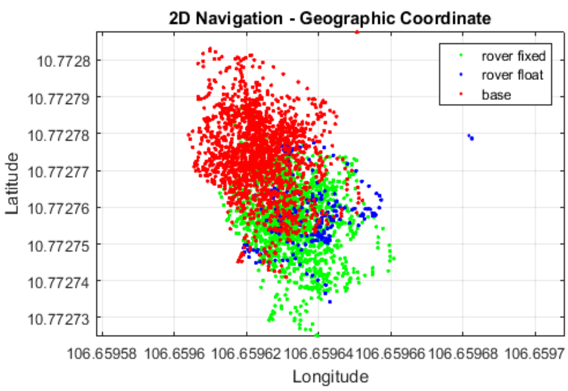

Figure 8. Estimation result in Earth's geographic coordinate.

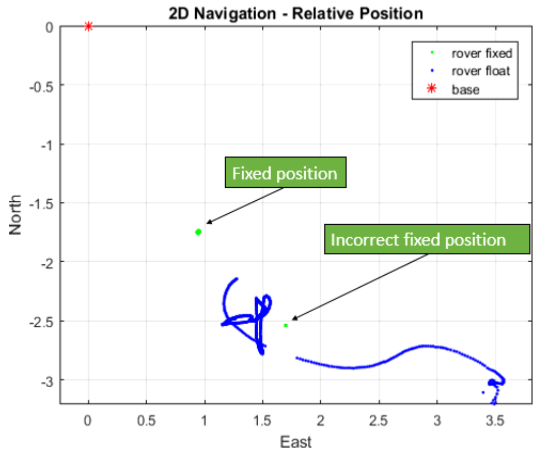

Figure 9. Relative pos. between antennas, the same dataset as Fig. 8.

B. *Dynamic Test*

Using the GPS-RTK system with dual-frequency GPS receivers, we have test results in the case of moving in Fig. 10 and Fig. 11. The amplitude of slider's trajectory is 50 centimeters peak-to-peak. The selected trajectory type is the sine wave whose frequency of 0.05Hz. We only calculate the error among the fixed solutions. All the float solutions are rejected. We can see that the dynamic test also has high accuracy like the static test. The measurement RMS error is about 0.237 degrees with a baseline ranging from 0.78 meters to 0.85 meters. The average baseline value is 0.81 meters. Compared to the case of static test, the error of dynamic test is larger.

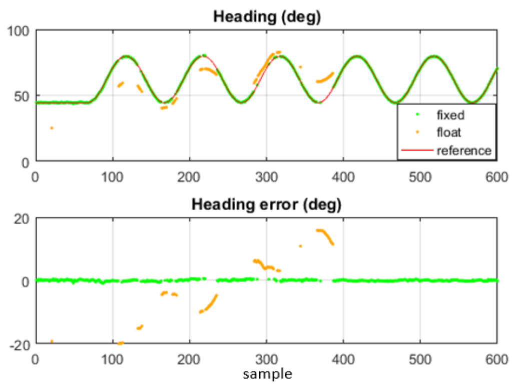

Figure 10. Heading angle and RMS error by time.

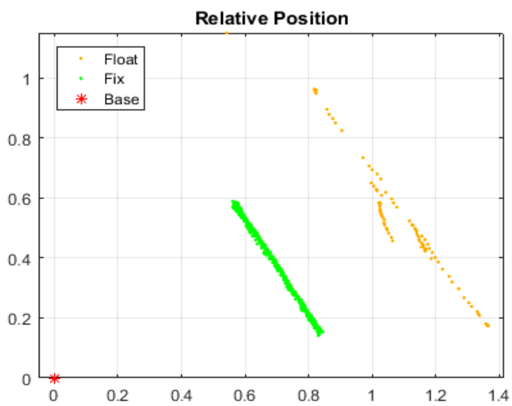

Figure 11. Relative position between antennas, dynamic test.

V. Conclusions

The paper has presented the heading estimation algorithm using dual-antenna GPS that applied on an ARM Cortex-M7 microprocessor. The static experiment results show that when the baseline is equal to 1 meter, the heading estimation accuracy is 0.27 degrees with single-frequency receivers and 0.16 degrees with dual-frequency receivers. In the dynamic test, the RMS error increases to about 0.29 degrees when the baseline is 1 meter, about twice as much as static test. The dual-frequency receiver has a much higher fixed solution rate than the single-frequency one (69% versus 60% on average). The accuracy of the measurement is proportional to the horizontal positioning error of the GPS position measurement and is inversely proportional to the distance between the two antennas. Compared to the system that uses the IMU to determine the heading angle, the dual-antenna GPS system is not affected by the magnetic field disturbance. However, the disadvantage is that it does not always introduce high-accuracy heading angle, the average fix rate is only from 60% to 70%. In the future, we will build an integrated GPS/INS navigation system with dual-antenna GPS that combines both sensors to take advantage of each system.

Conflict of Interest

The authors declare no conflict of interest.

Author Contributions

Tien-Dung Quoc Tran implemented the presented approach, conducted the experiments, analyzed the results and wrote the manuscript. Vinh-Hao Nguyen provided the original idea and gave critical feedback. All authors had approved the final version.

Acknowledgment

This research is funded by Ho Chi Minh City University of Technology - VNU-HCM under grant number To-DDT-2019-05.

References

[1] G. T. Schmidt and R. E. Phillips, "INS/GPS integration architectures," *NATO RTO Lecture Series, RTO-EN-SET-116, Low-Cost Navigation Sensors and Integration Technology*, 2010.

[2] D. M. Ma, J. K. Shiau, I. C. Wang, and Y. H. Lin, "Attitude determination using a MEMS-based flight information measurement unit," *Sensors*, vol. 12, pp. 1-23, 2012.

[3] Eun-Hwan Shin, "Accuracy improvement of low cost INS/GPS for land applications," The University of Calgary, 2001.

[4] M. B. Alatise and G. P. Hancke, "Pose estimation of a mobile robot based on fusion of IMU data and vision data using an extended Kalman filter," *Sensors*, vol. 17, pp. 2164, 2017.

[5] M. T. K. Tsun, B. T. Lau, and H. S. Jo, "Exploring the performance of a sensor-fusion-based navigation system for human following companion robots," *International Journal of Mechanical Engineering and Robotics Research*, vol. 7, no. 6, pp. 590-598, 2018.

[6] Y. Gao, S. Liu, M. M. Atia, and A. Noureldin, "INS/GPS/LiDAR integrated navigation system for urban and indoor environments using hybrid scan matching algorithm," *Sensors*, vol. 15, pp. 23286-23302, 2015.

[7] Antonio Angrisano, "GNSS/INS Integration Methods," 2010.

[8] M. Strohmeier and S. Montenegro, "Coupled GPS/MEMS IMU attitude determination of small UAVs with COTS," *Electronics*, vol. 6, p. 15, 2017.

[9] A. Consoli, J. Ayadi et.al., "A multi-antenna approach for UAV's attitude determination," *IEEE Metrology for Aerospace (MetroAeroSpace)*, Benevento, Italy, 2015.

[10] N. Nadarajah, P. J. Teunissen, and N. Raziq, "Instantaneous GPS-Galileo attitude determination: Single-frequency performance in satellite-deprived environments," *IEEE Transactions on Vehicular Technology*, 2013.

[11] P. Henkel and C. Guenther, "Attitude determination with low-cost GPS/INS," *The 26-th ION GNSS*, Nashville, TN, USA, 2013.

[12] C. Eling, L. Klingbeil, and H. Kuhlmann, "Real-time single-frequency GPS/MEMS-IMU attitude determination of lightweight UAVs," *Sensors*, vol. 15, pp. 26212-26235, 2015.

[13] T. Takasu, *RTKLIB ver. 2.4.2 Manual*, 2013.

[14] P. Teunissen, "The least-squares ambiguity decorrelation adjustment: A method for fast GPS ambiguity estimation," *Geodesy*, vol. 70, pp. 65-82, 1995.

[15] X. W. Chang, X. Yang, T. Zhou, "MLAMBDA: A modified LAMBDA method for integer least-squares estimation," *Geodesy*, vol. 79, pp. 552-565, 2005.

Tien-Dung Quoc Tran received B.S. degree in electrical and electronics engineering from the Ho Chi Minh city University of Technology, Vietnam in 2018. He is currently a member of Department of Control and Automation, Ho Chi Minh city University of Technology. His research interest is multi-sensor integrated system for navigation and mapping.

Vinh-Hao Nguyen is presently a lecturer of Electrical and Electronics Engineering at Ho Chi Minh city University of Technology, Vietnam. He received B.S. and M.S. degrees in Electrical and Electronics Engineering from Ho Chi Minh city University of Technology, Vietnam, in 2001 and 2003, respectively. He received Ph.D. degree in Electrical Engineering from the University of Ulsan, Korea, in 2009. His research interests are INS/GPS positioning system, autonomous robot, adaptive control systems. His research interests are INS/GPS positioning system, autonomous robot, adaptive control systems.